Introduction to WFPC Photometry

John A. Biretta[1], Sylvia M. Baggett[1], John W. MacKenty[1],
Christine E. Ritchie[1] and William B. Sparks[1]

Abstract

We briefly review photometric analysis and calibration of WFPC images. We discuss absolute calibration using SYNPHOT, and various photometric problems peculiar to WFPC data.

I. Introduction

This paper provides a brief introduction to photometric analysis of *HST* Wide-Field Planetary Camera data. We review a number of resources available to aid photometric analysis, and describe various problems and solutions peculiar to WFPC data. The measurement of raw counts on the images is severely impacted by the spherically aberrated PSF, but PSF fitting and core aperture photometry appear to offer effective solutions. The SYNPHOT synthetic photometry package provides a powerful tool for absolute photometric calibration; we briefly describe its ingredients and usage. A number of problems compromise photometric accuracy. Most of these are rooted in either contamination (throughput variations, measles, scattered light), the use of earth flats (ND filter patterns and residual streaks), or PSF variations (with time and field position). Most of these problems can be minimized or eliminated with some effort.

II. Extraction of Photometric Information from Images

The extraction of photometric information is made difficult by the spherical aberration and the resulting point spread function (PSF) wings. The PSF core, defined to be 0.2 arcseconds in diameter, contains only about 15 percent of the light for a stellar source. A much larger aperture 4 or 5 arcseconds in diameter must be used to measure all the light (Figure 1). Hence there are several competing factors: one would like to measure only the PSF core in order to maximize the signal-to-noise ratio, minimize crowding problems, and ease background subtraction. But on the other hand, a large aperture encircling all the light is required to guarantee photometric accuracy.

Two methods for extracting photometric information have been successfully applied to WFPC images – PSF fitting and core aperture photometry. PSF fitting uses a model PSF and least squares fitting to determine total counts and positions of stellar

1. Space Telescope Science Institute, Baltimore, MD 21218

objects. The model PSF can be either an analytic function or an empirical function extracted from the image itself. Galaxies can be fit also by convolving an appropriate galaxy model with the model PSF before fitting to the image. For this method the signal-to-noise ratio is automatically optimized by choosing an appropriate weighting function for the image pixels. Crowded fields can be dealt with by simultaneously fitting overlapping objects, and the sky level can be simply included in the fit. There are several popular software packages for PSF fitting. The DAOPHOT package by Stetson is described in another paper in this volume. Another package, DoPHOT (Schechter, Mateo, Saha 1993) includes iterative object classification with analytic PSF fitting. The accuracy of this method will generally be limited by the accuracy of the model PSF.

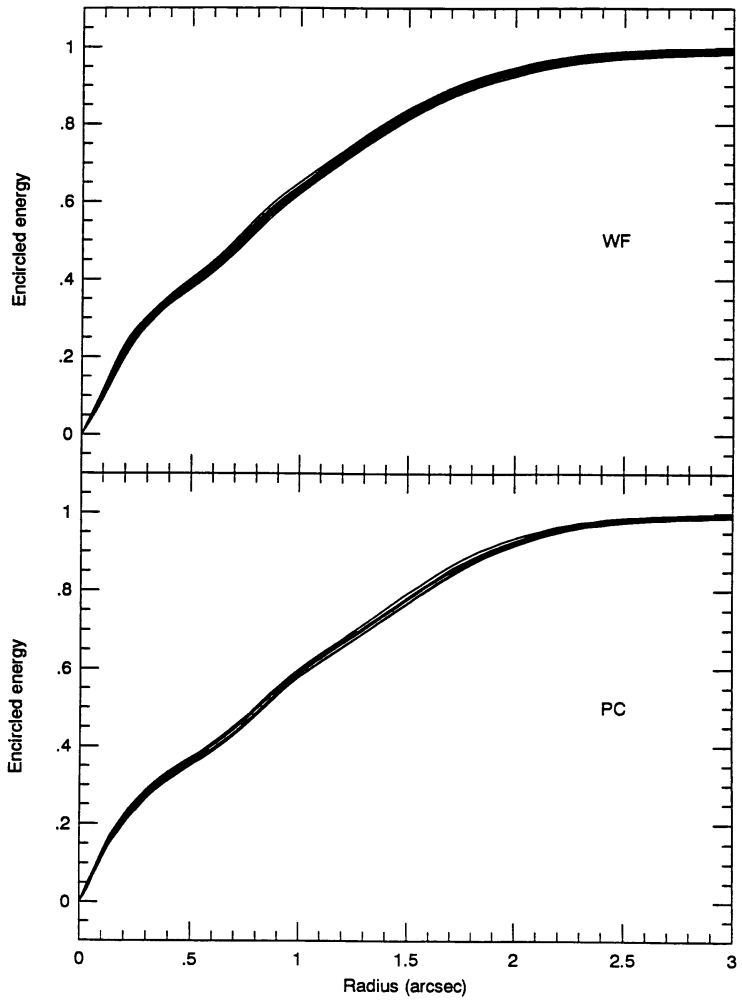

Figure 1: Plots showing encircled energy as a function of aperture radius for the Wide Field (top) and Planetary (bottom) Cameras. From Holtzman (1992).

Core aperture photometry involves measuring only the counts within the PSF core (<0.2 arcsecond radius aperture), and then later correcting the core counts to a larger aperture. The correction may be determined empirically from measurements on bright stars in uncrowded fields, or from measurements on model PSFs. The use of a small aperture serves to both optimize the signal-to-noise ratio and minimize

crowding problems. The accuracy will be limited both by undersampling of the observed PSF by the detector pixels (especially for WFC data), and by variations in the ratio of PSF core light to PSF total light (see section 4 below).

The PSF fitting and core aperture photometry have been shown to give results consistent to about 0.06 magnitudes on bright stars (m<18.5), and a little poorer on faint ones, for the Wide Field Camera (Gilmozzi 1990).

At this point it is appropriate to mention the WFPC PSF library. A library of over 900 observed PSFs is maintained in the Calibration Data Base System (CDBS), which may be accessed through the normal data archive retrieval system. These are short exposures of single bright stars, and cover most of the area of WF2 and the four PC detectors. Most of the observations were made through the F555W and F785LP filters, but small amounts of data are available for twelve other filters. Detailed information on the PSF library is given in Baggett and Mackenty (1993). The TIM and Tiny Tim programs may also be used to compute model PSFs; these are reviewed in other papers in this volume.

III. Absolute Photometric Calibration with SYNPHOT

The SYNPHOT synthetic photometry program is part of the STSDAS package, and is originally based on the XCAL program by Keith Horne. It first derives an effective response function for the total *HST* + WFPC + filter system by multiplying together all the transmission and detection efficiency curves for the relevant components. This response function is then convolved with model spectra to predict observed count rates. Observations can then be calibrated by comparing the predicted and observed count rates for an appropriately chosen model spectrum.

The package is very powerful, in that it allows all possible observation modes to be crossed with a huge variety of model spectra. The *HST* and WFPC throughputs and efficiencies are derived from ground-based measurements which are adjusted to reflect the actual on-orbit performance. Model spectra available in the package include observed stellar spectra, as well as, model power-law, black body and polynomial spectra. The observed spectra include *HST* standard stars and atlases such as the Gunn-Stryker stellar spectral atlas. Other effects, such as reddening, may also be included in the model spectrum. Response curves for standard filter sets are included (e.g. Johnson U, B, V, R, I) so that model spectra may be scaled to arbitrary magnitudes on other systems.

The photometric calibration routinely provided in the calibration pipeline is based on the results of synthetic photometry with the SYNPHOT package. A rough calibration is placed in several keywords in the calibrated data binary header (part of the .C0D file); these keywords may be examined with the IMHEAD task in IRAF. This calibration is derived assuming a model spectrum having constant F_λ (defined in units erg cm^{-2} sec^{-1} $Angstrom^{-1}$). The instrument mode assumed for the SYNPHOT calculation is given by the PHOTMODE keyword (e.g PHOTMODE="PC,5,F,DN,F1042M,OPEN,CAL"), and should be identical to the mode used for the observation. The four keywords containing the resulting calibration are thus:

PHOTFLAM: inverse sensitivity, defined as F_λ (in units of erg cm^{-2} sec^{-1} Angstrom^{-1}) for a count rate of 1 DN sec^{-1}.
PHOTZPT: zero-point magnitude (Space Telescope Magnitude at F_λ=1).
PHOTPLAM: pivot wavelength for the filter in Angstroms.
PHOTBW: RMS filter bandwidth in Angstroms.

The Space Telescope Magnitude system (STMAG) is based on flux per unit wavelength, or units of F_λ, with the zero point set such that Vega has magnitude zero in the Johnson V passband.

```
cl> stsdas
st> hst_calib
hs> synphot
sy> calcphot counts wfpc,f555w "rn(bb(5000),band(v),18.6,vegamag)"
Number of modes = 1
Mode = wfpc,wf,2,f555w,cal
      Pivot          Equiv Gaussian
  Wavelength            FWHM
   5468.423             1199.32          wfpc,wf,2,f555w,cal
Spectrum:       rn(bb(5000),band(v),18.6,vegamag)
        E(B-V)          (COUNTS s^-1 hstarea^-1)
           0.                  412.4875
sy>
```

Figure 2: Sample SYNPHOT run for WFPC. Input format is appropriate for SYNPHOT version Nov. 1993. From Bushouse (1993)

Observers may also derive detailed calibrations which are tailored to their target spectra using SYNPHOT. Figure 2 shows a sample run of SYNPHOT program CALCPHOT which computes the expected count rate for a model spectrum. Once in the SYNPHOT package, the single command line "CALCPHOT ..." produces the output shown. Here a calibration is derived for observations made on detector WF2 using the F555W filter. The model spectrum is a 5000 degree Kelvin blackbody re-normalized to a magnitude V=18.6 in a system where Vega has V=0, and the result is a count rate of 418 DN $second^{-1}$. Observers should get a copy of the latest and greatest SYNPHOT manual by Bushouse (1993), and check that they have recent versions of the SYNPHOT photometry tables in their STSDAS installation.

We note that the keyword CAL must be specified in the OBSMODE when deriving SYNPHOT calibrations for flat fielded images. The absence of this keyword indicates the data are not flat fielded, and are in units of raw counts.

We now briefly discuss derivation of the SYNPHOT efficiency curves for WFPC. A more complete discussion is given by Sparks, Ritchie, and MacKenty (1992). The

SYNPHOT calibration is based on observations of the UV photometric standard star BD+75325, which were taken on 5 February 1992 immediately following a decontamination. This is sometimes referred to as the "baseline epoch for photometric calibration." Ten filters covering the range 1900 to 10400 Angstroms were used with detectors WF2 and PC6. Other ingredients to the calibration were ground-based measurements of the WFPC filter throughout curves and distributed quantum efficiencies (DQE) of all detectors, as well as measurements of the inter-chip flatfield corrections from on-orbit measurements. From these ingredients two sets of improved DQE curves were derived for all eight CCDs, one set applicable to un-flatfielded data, and one set applicable to fully calibrated data. These revised curves are incorporated in the current SYNPHOT tables. Some indication of the accuracy of this calibration is provided by the residual scatter in the sensitivities between different filters. This residual scatter is about 6 percent over all the CCDs at wavelengths longer than 3000 Angstroms, and somewhat less, about 4 percent, for data on WF2 and PC6. It is possible that improved flat fielding could reduce this scatter.

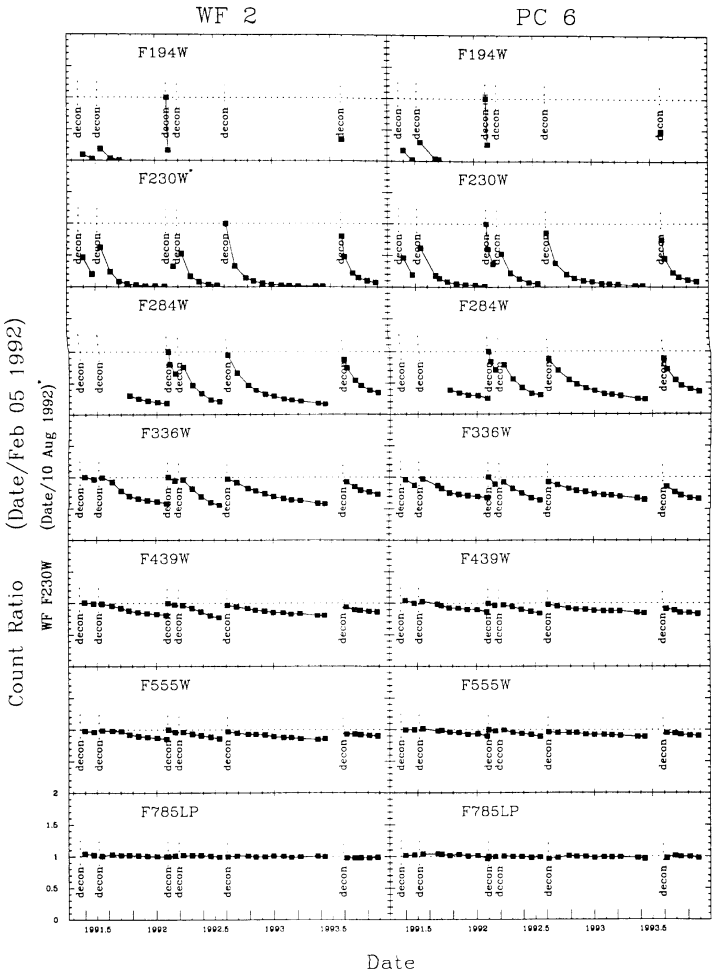

Figure 3: Relative throughput as function of time. Throughput is defined to be unity on 5 February 1992. The left set of panels show the center of WF2, while the right set show the center of PC6. Each small panel shows a different filter, with wavelength increasing from the top to bottom panels. Times of decontamination events are indicated by "decon." From Ritchie.

IV. Problems Limiting Photometric Accuracy

The WFPC SYNPHOT calibration assumes that all detector pixels have the same response as the centers of detectors WF2 and PC6 on 5 February 1992. Any factors which cause this to be untrue will impact the photometry. We now consider several specific effects which limit the accuracy of the photometry.

Time Dependent Throughput Variations

A quasi-uniform contamination layer builds up on the CCD windows between decontaminations. This molecular layer greatly reduces the instrumental throughput at UV and blue wavelengths. Weekly observations of a photometric standard star on WF2 and PC6 are made to track these variations, and typical results are shown in Figure 3. Since the SYNPHOT photometry and Figure 3 data are both relative to the same date, 5 February 1992, one can simply read the throughput reductions off the graph and apply them to calibrated data.

We will soon incorporate these throughput variations into SYNPHOT by adding the keyword CONT to the OBSMODE. For example:

OBSMODE = PC, 6, F555W, DN, CAL, CONT#49020

tells SYNPHOT to include appropriate throughput corrections for contamination on date MJD=49020 (Sparks and Ritchie 1994).

Flat Field Effects

Neutral Density Filter Pattern. The red-leak in the F122M filter has been used as a neutral density filter when taking many of the earth flats for broad band filters (e.g. filters F555W, F606W, F675W, F702W, F725LP, F814W, F850LP, etc.). This neutral density filter is non-uniform, and introduces a 30 percent peak-to-peak brightness gradient across all four WFC CCDs. Since this pattern appears in the flats, but not in the actual data, it introduces a corresponding error in the photometry. The Planetary Camera CCDs only view the center of this filter, so the effective gradient is only about 10 percent. There are also donuts where the flats are 2 percent too bright, which are cause by pinholes in the F122M filter.

These patterns introduced by the flats will have little effect on photometry for small targets at the WF2 and PC6 default aperture positions, since the standard stars are also observed there. But there can be a large impact on wide-field photometry. One solution is to derive the F122M filter pattern and then remove it from the images. The pattern can be derived by computing the ratio of narrow band filter flats observed with and without F122M, or by comparing the earth flats using F122M to sky flats.

The neutral density filter patterns also have some impact on the SYNPHOT baseline photometric calibration. The photometry observations on 5 February 1992 were calibrated using flats taken with and without the F122M (and also F8ND) filters, which, since the flats are normalized to unity, introduces a ~6 percent scatter in the

WFC photometric calibration data, and a somewhat smaller in the scatter in the PC. This scatter causes ~3 percent errors in the final photometric calibration, depending on the wavelength and CCD.

Residual Streaks in Earth Flats. The flat fields are derived from observations of the sunlit earth. In cases of short earth exposures (<1 sec) at red wavelengths, these flats will contain streaks caused by the combined effects of spacecraft motion and earth features. While specialized software is used to remove these streaks, it is not always successful, and residual streaks can appear in the flats. These residual streaks have an amplitude of a few percent in many filters, with the worst cases showing streak amplitudes of about 15 percent. The solution is to avoid short exposure earth flats, especially in the red and far-red. If none are available, one should consider using narrow band flats at nearby wavelengths, as these tend to have long exposures.

Short Exposure Reciprocity Effect. The CCD artifacts look different in exposures <1 second and >> 1 second. Apparently there is some change in the QE at very short exposures. The size of this effect is a few percent. The solution is to avoid using short exposure flat fields for long exposure images. This can be accomplished by using ND filters to observe the flats (which have other problems noted above), or use of sky flats, or by using narrow band flats at nearby wavelengths.

Persistent Measles. Decontaminations after February 1992 have been unable to remove all contaminants from the CCD windows. Contaminants consistent with 10 to 15 μm particles remain on the windows, and cause diffractive features (i.e. “persistent measles”) about 10 PC pixels in diameter to appear in the images. The amplitude of these features is about 1 percent in intensity for the WFC and most of PC6 in filter F555W. Larger errors, 2 to 5 percent, are seen on some of PC6 and over much of the other PC chips, with PC8 being the worst. The features are relatively stable, though some changes are seen across decontaminations. The easiest solution is to use DELTAFLATs to locate these features, and then decide if they will impact the target. The DELTAFLATs may also be used to correct the data, though this will only be partially successful, since the particles are out of focus. DELTAFLAT corrections will tend to be more successful on extended targets whose illumination pattern more closely matches the internal flats.

Scattered Light and Flat Field Edge Droop. Earth flats and internal flats taken when the windows are heavily contaminated (quasi-uniform layer) show flat field edge droop due to scattering of light by the contaminants. The flats appear bright in the centers, since the scattering angle is small and the photons are detected in nearby pixels. The flats are low at the edges since scattered photons fall outside the CCD detector. Most science data does not show this effect, since only small regions of the window are illuminated, and the scattered photons are simply lost into the background noise. Hence, the application of flats and DELTAFLATS can introduce errors into the data. These effects will cause errors up to about 8 percent at the CCD edges at 4000 Angstroms. At 5500 Angstroms the errors are less than 5 percent, and at 8000 Angstroms less than 1 percent. One can attempt to evaluate this effect for a given flat, by comparing internal flats near the time of the flat field observations, with those taken when the instrument is relatively uncontaminated.

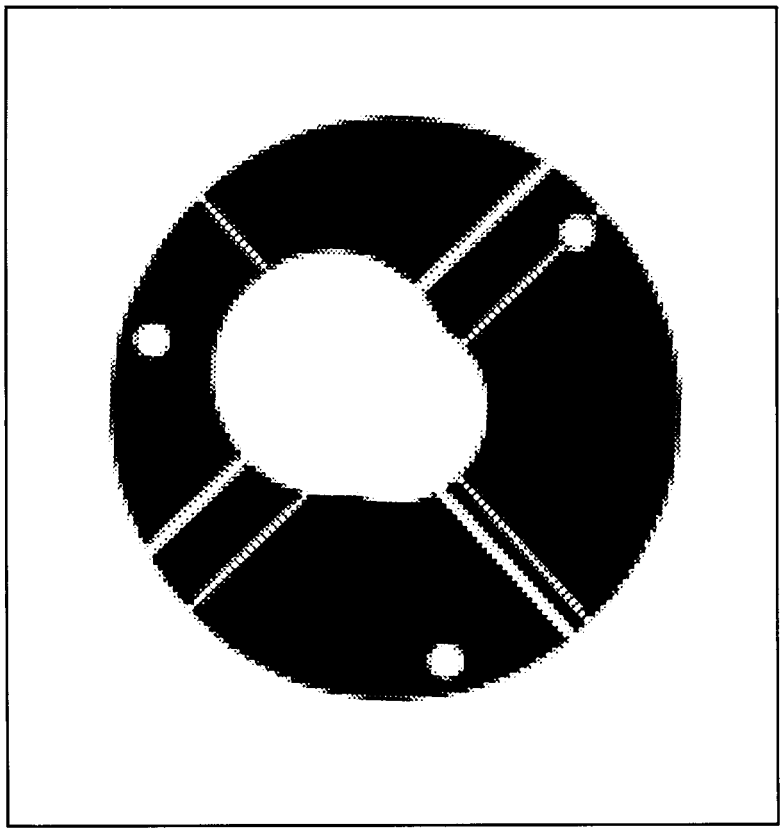

Figure 4: Effective OTA pupil seen by corner of typical WFC CCD. The large circular shadow of the camera secondary, together with its three support posts, have moved significantly off axis. From Holtzman 1992.

PSF Variations.

Variations in the Point Spread Function (PSF) will impact the extraction of photometric information from the images. The PSF varies with both detector position and time.

Variations with Field Position. The PSF varies across each CCD due to vignetting in the CCD camera repeater optics. This has several effects, one of which is to alter the intensity of the PSF core relative to the wings. In the centers of the CCDs, the shadow of the camera relay secondary mirror envelopes the telescope (OTA) secondary mirror shadow, so that the total obscuration is minimized. However, in the CCD corners, the shadow of the camera secondary moves off axis, so that a larger region near the center of the OTA primary mirror is obscured (Figure 4). Since the PSF core and wings are formed by different areas of the primary mirror, this vignetting will alter the relative intensity of the core and wings. (We note that while flat fielding does correct the reduction in *total counts* cause by this vignetting, it does not correct variations in the *relative intensities* of the PSF core and wings.) Variations are also seen in the detailed structure of the PSF wings (tendrils, etc.) as the camera secondary support shadows move and interact with other obscurations in the system.

Images also show a tendency for the PSF core to become elliptical away from the pyramid apex. These PSF variations must be addressed in order to obtain accurate photometry over a wide field of view. Variants of both DAOPHOT and DoPHOT are capable of handling spatially variable PSFs.

Variations with Time. Large changes in the PSF can occur at OTA focus adjustments, which are periodically made to compensate for shrinkage of the OTA mechanical structure. Small variations in the focus (as well as small position shifts) are also seen on time scales near the orbit period. This is sometimes referred to as OTA breathing and is believed to be caused by thermal expansion effects in the OTA. A final effect is that the solar array induced jitter can cause images to trail slightly. This primarily occurs at terminator crossings, but events elsewhere in the orbit are not unknown. These later two effects have short timescales, and will compromise comparison of PSFs on different data frames, or comparisons between data and model PSFs. For observations obtained in fine-lock tracking more, the Fine Guidance Sensor data can be used to derive a jitter map showing the pointing errors; this can in turn be used to alter the model PSF.

References

Baggett, S. B. and MacKenty, J. W. 1993, The WFPC Observed PSF Image Library, (WFPC Instrument Science Report 93-03, available from STScI Science Instruments Branch).

Bushouse, H. 1993, Synphot User's Guide, (available from STScI Science Software Branch).

Gilmozzi, R. 1990, Core Aperture Photometry with the WFPC, (WFPC Instrument Science Report 90-07, available from STScI Science Instruments Branch).

Holtzman, J. 1992, in WFPC Final Orbital / Science Verification Report, ed. S. Faber, (available from STScI User Support Branch).

Schechter, P. L., Mateo, M. L., and Saha, A., 1993, P.A.S.P. 105, 1342.

Sparks, W.B., Ritchie, C.E. and MacKenty, J.W. 1992, The Absolute Efficiency of the WFPC, (WFPC Instrument Science Report 92-09, available from STScI Science Instruments Branch).

Sparks, W.B., and Ritchie, C.E. 1994, Time Dependent Synphot Calibration, (WFPC Instrument Science Report 94-xx, available from STScI Science Instruments Branch), in preparation.